



Soft Matter

**Organic glasses with tunable liquid-crystalline order
through kinetic arrest of end-over-end rotation: The case of
saperconazole**

Journal:	<i>Soft Matter</i>
Manuscript ID	SM-ART-11-2019-002180.R1
Article Type:	Paper
Date Submitted by the Author:	20-Jan-2020
Complete List of Authors:	Chen, Zhenxuan; University of Wisconsin Madison, School of Pharmacy Yu, Jinguang; University of Wisconsin Madison, School of Pharmacy Teerakapibal, Rattavut; University of Wisconsin Madison, School of Pharmacy Meerpoel, Lieven; Janssen Pharmaceutica NV Richert, Ranko; Arizona State University, School of Molecular Sciences Yu, Lian; University of Wisconsin Madison, School of Pharmacy

SCHOLARONE™
Manuscripts

Organic glasses with tunable liquid-crystalline order through kinetic arrest of end-over-end rotation: The case of saperconazole

Zhenxuan Chen¹, Janguang Yu¹, Rattavut Teerakapibal¹, Lieven Meerpoel², Ranko Richert³,
Lian Yu^{1*}

¹School of Pharmacy, University of Wisconsin-Madison, Madison, Wisconsin 53705, USA

²Janssen Pharmaceutica NV, Turnhoutseweg 30, 2340 Beerse, Belgium

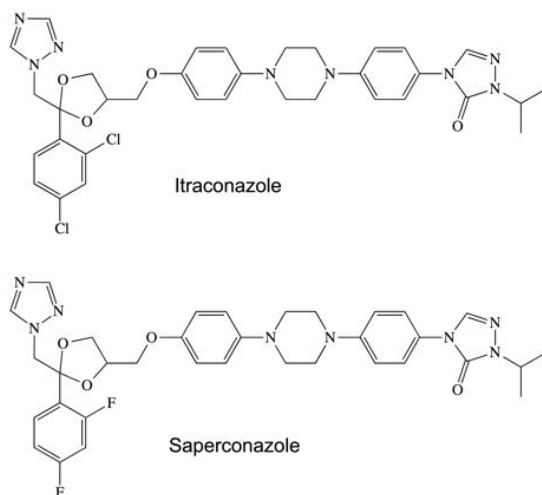
³School of Molecular Sciences, Arizona State University, Tempe, Arizona 85287-1604, USA

Abstract. Liquid crystals (LCs) undergo fast phase transitions, almost without hysteresis, leading to the notion that it is difficult to bypass LC transitions. However, recent work on itraconazole has shown that a nematic-to-smectic phase transition can be frustrated or avoided at moderate cooling rates. At each cooling rate, the highest smectic order obtained is determined by the kinetic arrest of the end-over-end molecular rotation. We report that the same phenomenon occurs in the system saperconazole, an analog of itraconazole where each of the two Cl atoms is replaced by F. Saperconazole has a wider temperature range over which smectic order can develop before kinetic arrest, providing a stronger test of the previous conclusion. Together these results indicate a general principle for controlling LC order in organic glasses for electronic applications.

Introduction

Liquid crystals (LCs) are remarkable materials. In contrast to ordinary liquids, molecules in LCs are highly organized in terms of their relative orientations and positions while maintaining fluidity. LC structures can be rapidly modified by temperature or external fields, allowing LCs to serve as displays and sensors. Upon cooling, a *thermotropic* LC transforms from an isotropic to a nematic and/or smectic structure. These transitions are often extremely fast and thus useful as temperature calibration standards at high cooling rates (up to 2×10^4 K/s).^{1,2} Many theories of LC transitions do not consider time as a variable, effectively treating them as instantaneous and thermodynamically rather than kinetically controlled.³⁻⁵

Despite the common notion that LC transitions are fast and easily reversible, recent work has shown that cooling at moderate rates can frustrate and even avoid LC transitions. For itraconazole, an antifungal medicine (Scheme 1), slow cooling of its liquid reveals the familiar transformations from an isotropic phase to a nematic phase and then to a smectic phase, while fast cooling (> 20 K/s) bypasses the nematic-smectic transition altogether.⁶ As a result, glasses can be prepared with a wide range of smectic order (including zero smectic order) simply by cooling at different rates. For this system, the smectic order trapped in the glass is the order reached by the smectic phase before the kinetic arrest of the end-over-end rotation of the rod-like molecule. In a LC, rod-like molecules tend to align in parallel with each other, causing the end-over-end rotation to be significantly slower (by a factor of 100 or more) than rotation about the long axis⁷⁻⁹ and to undergo kinetic arrest at a higher temperature at a given cooling rate. In related reports, different LC phases can be accessed by cooling at different rates,^{10,11} again demonstrating a kinetic control, as opposed to thermodynamic control, of LC transitions.



Scheme 1. Molecular structures of itraconazole and saperconazole.

To test the generality of the conclusion reached with itraconazole, we have studied its analog saperconazole (Scheme 1), obtained by replacing each of itraconazole's two Cl atoms by F. Like itraconazole, saperconazole is an antifungal agent¹² and forms LCs. With respect to its LC behavior, saperconazole has a wider temperature range over which LC order can develop before kinetic arrest (see below) and thus provides a stronger test of the previous conclusion on what controls the smectic order. We report that the smectic order in saperconazole can be continuously varied through cooling rate and is controlled by the kinetic arrest of the end-over-end rotation. Together with the previous itraconazole case, these results indicate a general principle for controlling LC order in organic glasses for applications in drug delivery and organic electronics.¹³⁻¹⁶

Experimental

Saperconazole was obtained from Janssen Pharmaceutica NV and used as received. Similar to itraconazole, saperconazole is a racemic mixture of 4 *cis* isomers (a *cis* isomer is defined with respect to the two chiral centers on the dioxolane ring, with the phenyl group at one center and the H atom at the other residing on the same side of the ring).

Differential Scanning Calorimetry (DSC) was performed with a TA 2000 unit. In a typical run, a 5 mg sample was heated and cooled in an aluminum pan at controlled rates to determine the temperatures of LC transitions and of the glass transition.

X-ray scattering was performed in the transmission geometry with a Bruker SMART APEX2 diffractometer. A capillary tube (Charles Supper, MA, 0.7 mm OD, 10 μm wall thickness) containing a sample was irradiated perpendicularly by an X-ray beam from a $\text{Cu } K_{\alpha}$ source with a 0.5 mm diameter beam. Scattered X-ray was detected with a 2D detector located 12 cm away from the sample. Temperature was controlled during measurement with an Oxford 700 Cryostream to within 0.1 K. Crystalline saperconazole powder was loaded into the tube, which was then flame-sealed. The crystals were melted (m.p. 462 K) to produce the liquid sample for X-ray analysis. Glasses were prepared by cooling an isotropic liquid (above 381 K) at rates ranging from 0.01 to 180 K/s and their X-ray scattering was measured at 298 K. Cooling rates slower than 3 K/s were obtained using a Linkam microscope hot/cold stage or the sample cell of the DSC. The cooling rate of 20 K/s was obtained by plunging a molten sample in a capillary tube at 480 K into an ice/water bath. The cooling rate was measured by performing the same cooling procedure with a thin thermocouple inserted into the capillary tube. The fastest cooling (180 K/s) was achieved as follows: evaporate 1 ml of chloroform solution of saperconazole (2 mg/ml) to produce a film ~ 2 μm thick on a 3 cm \times 3 cm \times 0.05 mm sheet of Kapton, melt the sample on a Kofler Hot Bench, and plunge it into liquid nitrogen. The cooling rate was measured by performing the same cooling procedure with a thermocouple attached to the Kapton film. Vitrified saperconazole was scraped off the Kapton film and filled into a capillary tube for X-ray analysis.

Samples for dielectric spectroscopy were prepared by melting saperconazole onto a 30 mm diameter polished brass disk electrode of a liquid cell, adding a 25 μm thick polyimide spacer ring with 14 mm ID, and covering the sample and spacer with a second electrode of 20 mm diameter. With this capacitor mounted in the sample holder, saperconazole was melted at 500 K and slap-cooled to 300 K, before placing the sample in the cryostat. Measurement temperature was controlled with a nitrogen-gas cryostat and a Novocontrol Quatro controller to within 0.1 K. Frequency-dependent dielectric permittivity ϵ' and loss ϵ'' were measured using a Solartron SI-1260 unit equipped with a Mestec DM-1360 transimpedance amplifier.

Results and Discussion

Fig. 1 (top) shows the DSC traces of saperconazole. Upon cooling at 10 K/min, an isotropic liquid of saperconazole transforms to a nematic phase at $T_{N/I} = 381$ K (onset) and then to a smectic phase at $T_{Sm/N} = 366$ K (onset). At $T_{N/I}$, an ordinary clear liquid becomes cloudy and birefringent, as expected. At $T_{Sm/N}$, a change of optical properties also occurs and X-ray scattering confirms formation of smectic layers (see below). Upon further cooling, the system undergoes a liquid-to-glass transition with an onset at $T_g = 320$ K and a drop of heat capacity. Upon reheating, all the above transitions are reversed, with the exception that crystallization occurs above $T_{N/I}$. All the transitions above have been observed in the previously studied itraconazole (Fig. 1, bottom). One key difference between two systems is the faster crystallization of saperconazole. In fact, to observe its LC transitions without overlap with crystallization, the heating rate was increased to 50 K/min.

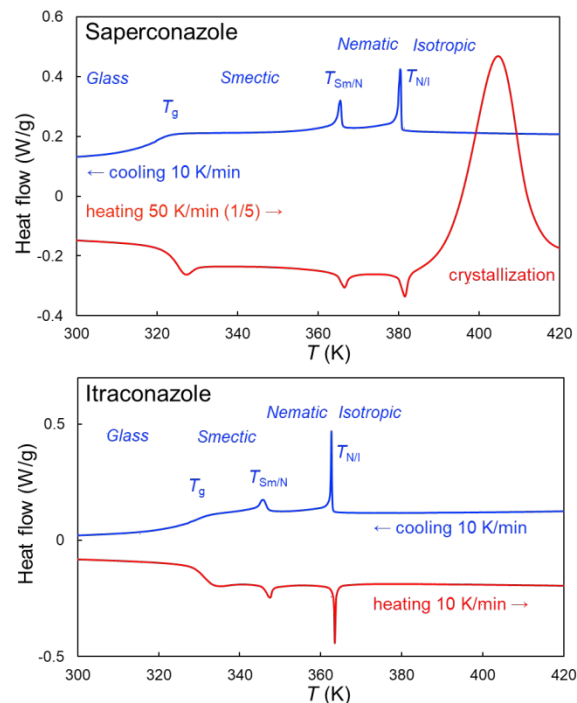


Figure 1. DSC traces of saperconazole (top) during cooling at 10 K/min and reheating at 50 K/min (signal reduced by a factor of 5), and of itraconazole (bottom) during heating and cooling at 10 K/min.

Aside from faster crystallization, saperconazole has a wider temperature range between the LC transitions and the glass transition relative to itraconazole. This implies that LC order can develop over a wider temperature range before kinetic arrest, providing a stronger test of the previous conclusion based on itraconazole.

Fig. 2a shows the X-ray scattering of saperconazole at several temperatures between T_g and $T_{Sm/N}$. In this range, the system is an equilibrium liquid in the smectic phase. The sharp peaks at 0.2 and 0.4 \AA^{-1} indicate the smectic order. The 0.2 \AA^{-1} peak results from periodic layers with a spacing of 3 nm, the length of the molecule,¹⁷ while the peak at 0.4 \AA^{-1} is the second-order diffraction of the layers. As expected for an equilibrium smectic liquid,¹⁸ the scattering intensity is temperature dependent (increases with cooling), but is independent of the path by which a given temperature is reached. The latter feature is shown by the inset of Fig. 2a where the temperature 328 K was reached by heating or cooling, without influence on the scattering peak. In addition to the sharp peaks at 0.2 and 0.4 \AA^{-1} , broad features are observed just to the right of each sharp peak and at 0.7 \AA^{-1} . These broad peaks arise from the excluded volume effect that exists even in the absence of LC order.¹⁸ For each rod-like molecule, the van der Waals volume is not penetrated by neighboring molecules and this leads to a positional order of the molecular centers of mass that reflects the molecular shape. Similar X-ray scattering features, both sharp and broad, have been observed in itraconazole.^{6, 19}

Fig. 2b shows the intensity (peak area) of the primary smectic scattering peak at 0.2 \AA^{-1} as a function of temperature. In this plot, the experimental intensity I is normalized by a constant I_0 obtained by model fitting [see eq. (1) below] so that the ratio I/I_0 represents the smectic order.²⁰ Measurements have been made both during cooling (solid symbols) and during heating (open symbols) in the temperature range $T_g < T < T_{Sm/N}$. In this range the system is in equilibrium and we observe good agreement between the cooling and heating results in this region, as expected. These results show that below $T_{Sm/N}$, smectic order rises steadily with cooling until T_g is reached. Below T_g , the system undergoes kinetic arrest, halting the rise of smectic order. A notable difference between itraconazole and saperconazole is that the latter crystallizes rapidly and its smectic phase could not be measured above $T_{Sm/N}$ using the current instrument to observe the complete loss of smectic order. Nevertheless, the available data are sufficient to model smectic ordering, as shown below.

The temperature dependence of the smectic scattering intensity of saperconazole is well described by:²⁰

$$I = I_0 \left[\frac{T_{Sm/N} - T}{T_{Sm/N}} \right]^x \quad (1)$$

where I_0 is a normalization constant, and x is an exponent between 0 and 1 describing how fast smectic order increases with cooling below $T_{Sm/N}$. According to Ref.²⁰, the amplitude of density modulation of the smectic layers is given by: $\Sigma = (I/I_0)^{1/2}$, with $\Sigma = 1$ corresponding to “perfect” smectic order in the absence of thermal fluctuation. The curve in Fig. 2b is a fit to the data using eq. (1). For this fit, $T_{Sm/N}$ is fixed at the DSC value (366 K). This fit yields $x = 0.64$, a value close to itraconazole’s $x = 0.67$, indicating smectic order grows at similar rates with cooling below $T_{Sm/N}$ in the two systems. The fitting also yields the parameter I_0 used to normalize the experimental intensity in Fig. 2b.

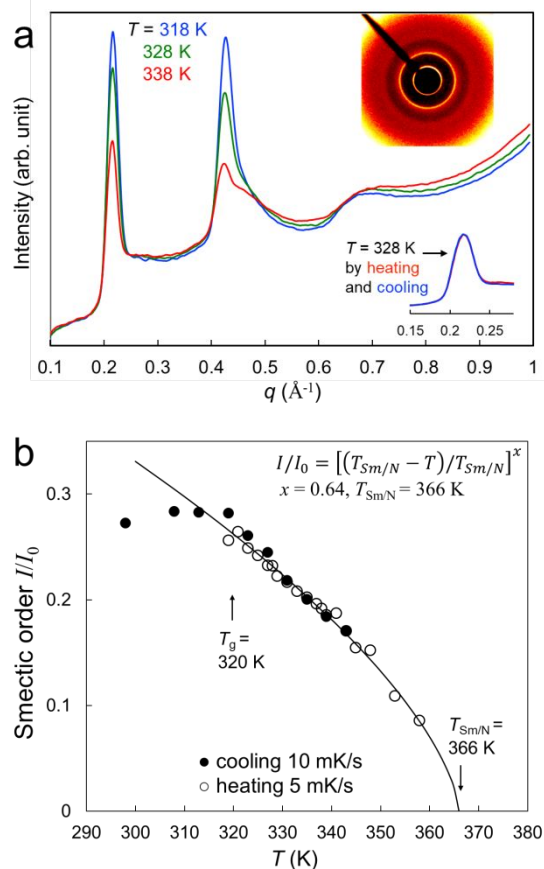


Figure 2. (a) Smectic scattering pattern of an equilibrium smectic liquid as a function of temperature during a heating run. The inset shows identical scattering intensity at 328 K reached by heating and cooling. (b) Normalized smectic scattering intensity vs. temperature. Agreement between the results of cooling (solid circles) and heating (open circles) runs indicates measurement of the equilibrium smectic order. The curve is a fit to eq. (1).

It is possible to vary the smectic order in saperconazole glasses considerably by cooling at different rates. Fig. 3a shows the X-ray scattering patterns of saperconazole glasses prepared at cooling rates ranging from 0.05 to 180 K/s. With increasing cooling rate, smectic scattering becomes weaker, indicating a loss of smectic order. At the fastest rate used, the sharp peaks at 0.2 and 0.4 \AA^{-1} are nearly absent, with their maxima shifting to the right and merging into the broad “excluded volume” peaks that are present even in the absence of LC order.¹⁸ All these features are analogous to the itraconazole case,⁶ with the difference that at the same cooling rate, saperconazole achieves higher smectic order than itraconazole or equivalently, requires faster cooling to reach the same order (see below).

Fig. 3b shows the cooling rate dependence of the smectic order of a saperconazole glass. Again, the experimental scattering intensity has been normalized by the value I_0 obtained by fitting the scattering intensity in the equilibrium liquid state to eq. (1). Note that faster cooling results in lower smectic order. Increasing the cooling rate from 0.01 to 180 K/s decreases the smectic scattering by a factor of 5. The two curves in Fig. 3b are two model predictions based on the kinetic arrest of different molecular motions to be discussed later.

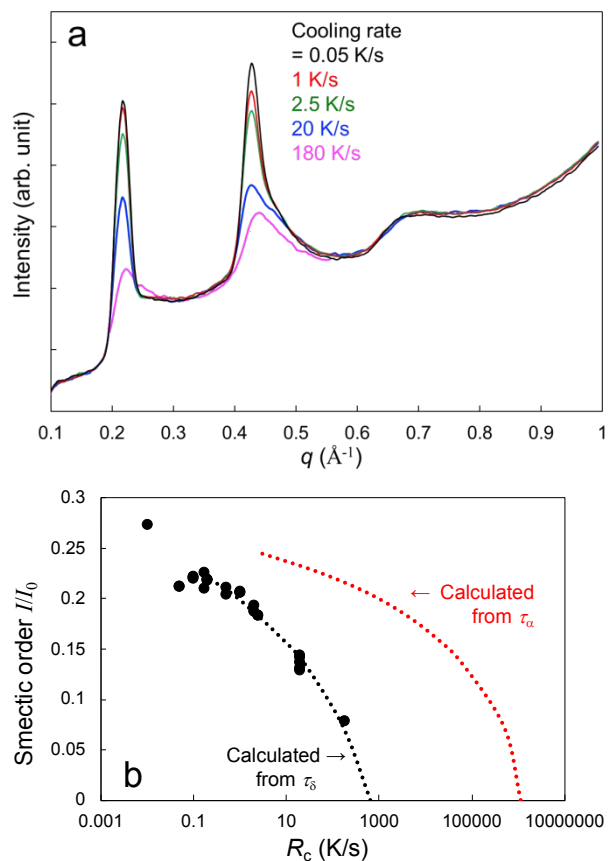


Figure 3. (a) X-ray scattering patterns of SAP glasses prepared at different cooling rates and measured at 298 K. Faster cooling leads to lower smectic order. (b) Normalized smectic scattering intensity at 0.2 \AA^{-1} , I/I_0 , as a function of cooling rate. The curves are predictions based on the kinetic arrest of different relaxation modes (α and δ).

To understand why the cooling rate influences smectic order in a saperconazole glass, the timescales of molecular rotations were measured by dielectric spectroscopy.⁷ Fig. 4a shows the typical dielectric loss spectra $\varepsilon''(\nu)$ of saperconazole as a function of temperature. With heating, the loss peak shifts to higher frequencies, as expected. Fig. 5 presents the relaxation times extracted from these spectra. In Fig. 4a, a slight decrease of signal is seen at high temperatures. This is due to crystallization, which reduces liquid volume but otherwise has no influence on the determination of liquid dynamics. Because of fast crystallization, both cooling and heating runs were performed to expand the temperature range of these measurements. The heating and cooling runs yielded consistent results and both are presented in Fig. 5 without distinction.

As in the case of itraconazole⁷ and other LC systems,^{8, 9} dielectric spectroscopy reveals two relaxation processes in saperconazole. This is illustrated in Fig. 4b using the spectrum at 360 K. The more intense relaxation peak occurs at higher frequency and a secondary peak is detected at lower frequency. Consistent with the literature, we term the main (fast) relaxation mode the α process and assign it to molecular rotation about the long axis, and term the weaker (slow) mode the δ process and assign it to molecular rotation about the short axis.

The two relaxation processes are modeled by the sum of a Havriliak-Negami (HN) and a Cole-Cole (CC) type dielectric functions plus a DC-conductivity term.²¹ Each total function has the form:

$$\varepsilon^*(\omega) = \varepsilon'(\omega) - i\varepsilon''(\omega) = \varepsilon_\infty + \frac{\Delta\varepsilon_\alpha}{[1 + (i\omega\tau_\alpha)^\alpha]^\gamma} + \frac{\Delta\varepsilon_\delta}{1 + (i\omega\tau_\delta)^\beta} + \frac{\sigma_{dc}}{i\omega\varepsilon_0}, \quad (2)$$

where ε_∞ is the dielectric constant in the high frequency limit and $\Delta\varepsilon$ is the relaxation strength with $\varepsilon_s = \varepsilon_\infty + \Delta\varepsilon_\alpha + \Delta\varepsilon_\delta$ being the static dielectric constant. The HN exponents α and γ ($0 < \alpha, \alpha\gamma \leq 1$) quantify the symmetric and asymmetric broadening of the α peak, respectively. The CC exponent β gauges the symmetric broadening of the δ peak. The value of σ_{dc} quantifies the level of DC-conductivity. Fig. 4b shows that eq. (2) gives an excellent fit of the observed spectrum. The main (fast) process is characterized by $\alpha = 0.72$ and $\gamma = 0.40$; the weaker (slow) process is characterized

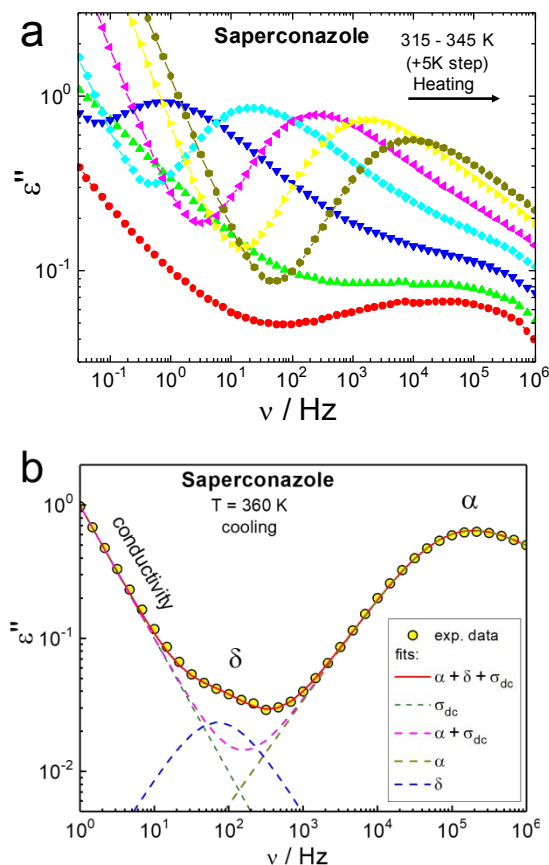


Figure 4. (a) Dielectric loss ε'' versus frequency ν at various temperatures. The main relaxation peak shifts to higher frequency with heating. The rising signal at low frequency is due to DC conductivity. The slight decrease of peak height at high temperatures is due to crystallization. (b) Two relaxation modes (α and δ) in saperconazole illustrated by the spectrum at 360 K. Two HN functions plus DC conductivity give excellent fit of the observed spectrum.

by $\beta = 0.90$. Thus the slow process is almost a Debye process, with only a slight symmetrical broadening. After accounting for the extent of crystallization, the strength of the main process is estimated to be $\Delta\varepsilon_\alpha \approx 4$. The slow process has $\sim 2.5\%$ of the relaxation strength of the fast process, with the percentage falling slightly with cooling (from 3.7% at 345 K to 1.7% at 330 K). Similar relative strengths have been reported for the two relaxation modes of itraconazole.⁷

We are now in a position to test the hypothesis that the smectic order obtained at a given cooling rate is controlled by the kinetic arrest of the end-over-end molecular rotation. The existence of two relaxation modes (τ_α and τ_δ) implies two glass transition temperatures ($T_{g\alpha}$ and $T_{g\delta}$) for a given cooling rate. For a cooling rate R_c , T_g is given by:

$$\tau(T_g) R_c = C \quad (3)$$

where $\tau = \tau_\alpha$ or τ_δ and C is a constant dependent upon the manner in which T_g is defined (the onset, the midpoint, or the endpoint of the glass transition; measured during heating or cooling).^{22, 23} The value of $C = 0.4\text{ K}$ holds for itraconazole and indomethacin when T_g is defined as the onset of DSC T_g during cooling and when τ is associated with the fast relaxation process τ_α .^{24, 25} For saperconazole, we find that the same C is valid. In Fig. 5, the dependence of the DSC T_g on the cooling rate R_c is plotted using the x axis for T_g and the secondary y axis for R_c . After relating the two y axes by eq. 3 with $C = 0.4\text{ K}$, the T_g data points connect smoothly with the τ_α data. This agrees with the previous result on LC systems that the DSC T_g is associated with the α process (rotation about the long axis)⁹ and validates eq. (3) for saperconazole. According to eq. (3), at an arbitrary R_c , the T_g for the α process can be read off from the τ_α curve at the intersection with the horizontal line $y_2 = R_c$, as shown in Fig. 5. We assume that eq. (3) holds for both relaxation modes, and this allows $T_{g\delta}$ to be evaluated as well.

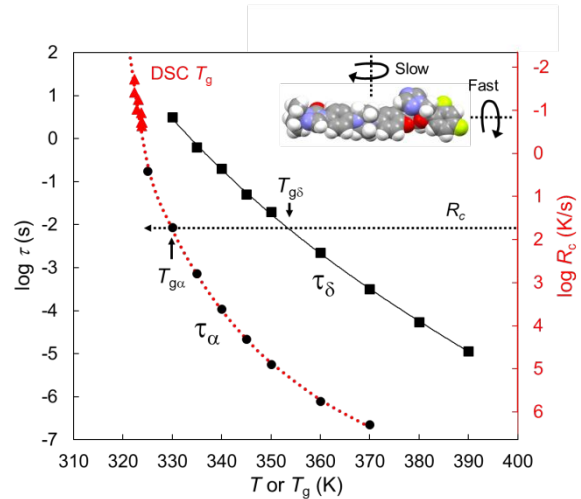


Figure 5. Two relaxation modes of saperconazole, τ_α (fast) and τ_δ (slow), The two modes correspond to molecular rotation about the long axis and the short axis of the molecule, as illustrated by the inset. Each relaxation time can be represented by a VFT function: $\log \tau = A + B/(T-T_0)$, where $A = -11.0$, $B = 332.6\text{ K}$, $T_0 = 292.6\text{ K}$ for τ_α , and $A = -15.0$, $B = 1759\text{ K}$, $T_0 = 216.7\text{ K}$ for τ_δ . The DSC T_g (onset) during cooling is plotted as solid triangles against cooling rate shown on the right y axis. The two y axes are related by eq. 3 with $C = 0.4\text{ K}$.

According to our hypothesis, the smectic order obtained at a given cooling rate is the order reached by the equilibrium liquid at $T_{g\delta}$; that is, $I = I_0 \left[\frac{T_{Sm/N} - T_{g\delta}}{T_{Sm/N}} \right]^{0.64}$. This provides a prediction of smectic order for any cooling rate *without adjustable parameter*. In Fig. 3b, this prediction is compared with experimental data, and we see an excellent agreement between the two. Fig. 3b also shows an alternative prediction (red curve) based on the assumption that smectic order is determined by the kinetic arrest of rotation about the long axis at $T_{g\alpha}$. This second prediction clearly deviates from experiment. Thus, the smectic order in saperconazole is controlled by the kinetic arrest of the slow, end-over-end rotation. This confirms the previous conclusion drawn with itraconazole.⁶

In Fig. 6 we compare the smectic ordering in itraconazole and saperconazole. In the equilibrium smectic phase, the two systems develop smectic order at similar rates when cooled below $T_{Sm/N}$ (Fig. 6a); however, because of its lower T_g relative to $T_{Sm/N}$ (Fig. 1), saperconazole can develop higher smectic order before kinetic arrest. For both systems, the smectic order trapped in a glass is a function of cooling rate (Fig. 6b). At the same cooling rate, saperconazole reaches higher smectic order than itraconazole, reflecting the lower temperature $T_{g\delta}$ at which its end-over-end rotation is frozen. This means that faster cooling is needed to fully eliminate smectic order in saperconazole than in itraconazole. The critical cooling rate is ~ 20 K/s for itraconazole and is estimated to be ~ 1000 K/s for saperconazole (Fig. 6b). Together the results on both systems offer a strong test of our hypothesis and the fact that both systems pass this test provides a strong support for the general principle that smectic order can be controlled through the kinetic arrest of the end-over-end molecular rotation.

Conclusions

Contrary to the common notion that it is difficult to frustrate or bypass LC transitions, the smectic order in saperconazole can be significantly changed by cooling at different rates. The phenomenon is fully analogous to that previously observed with the related compound itraconazole. For both systems, the kinetic arrest of the end-over-end rotation controls the smectic order obtained at a

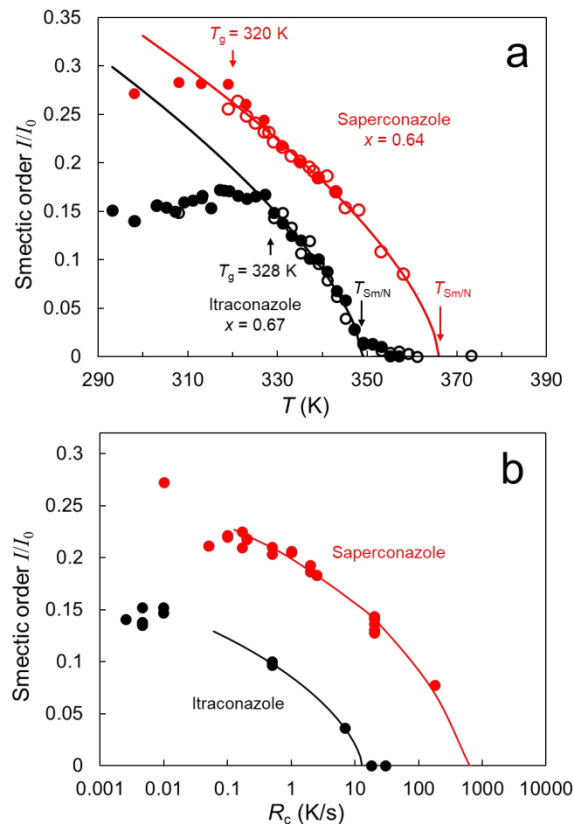


Figure 6. Comparison of smectic ordering in itraconazole and saperconazole. (a) Smectic order vs temperature. In each system, smectic order grows with cooling below $T_{Sm/N}$ until kinetic arrest (plateau). The curves are fits of the smectic order in the equilibrium smectic phase to eq. (1). (b) Effect of cooling rate on the smectic order trapped in the glass. The curves are predictions based on the kinetic arrest of the end-over-end rotation.

given cooling rate. Saperconazole provides a more rigorous test of the conclusion because of its wider temperature range in which smectic order can grow before kinetic arrest. Together the results on the two systems indicate a general principle to systematically control LC order in organic glasses for electronic applications. Future progress in this area will benefit from the testing of additional LC systems, including discotics, and other methods of kinetic arrest (e.g, solvent evaporation and vapor deposition). Also of interest is the stability of smectic order in the glassy state and the manner in which the system evolves toward the equilibrium smectic order.

Conflicts of interest

There are no conflicts to declare.

Acknowledgements

This work was supported by the National Science Foundation under Grant No. DMR-1904601. The authors thank Janssen Pharmaceutica NV for supplying saperconazole as well as the Molecular Structure Laboratory at University of Wisconsin-Madison and I. Guzei for assistance in collecting X-ray scattering data.

References

1. S. Wouters, F. Demir, L. Beenaerts and G. Van Assche, *Thermochimica acta*, 2012, **530**, 64-72.
2. J. Jiang, E. Zhuravlev, Z. Huang, L. Wei, Q. Xu, M. Shan, G. Xue, D. Zhou, C. Schick and W. Jiang, *Soft Matter*, 2013, **9**, 1488-1491.
3. W. Maier and A. Saupe, *Zeitschrift für Naturforschung A*, 1958, **13**, 564-566.
4. W. L. McMillan, *Physical Review A*, 1971, **4**, 1238.
5. P. G. de Gennes, *Solid State Communications*, 1972, **10**, 753-756.
6. R. Teerakapibal, C. Huang, A. Gujral, M. D. Ediger and L. Yu, *Physical review letters*, 2018, **120**, 055502.
7. M. Tarnacka, K. Adrjanowicz, E. Kaminska, K. Kaminski, K. Grzybowska, K. Kolodziejczyk, P. Wlodarczyk, L. Hawelek, G. Garbacz, A. Kocot and M. Paluch, *Physical Chemistry Chemical Physics*, 2013, **15**, 20742-20752.
8. A. Schonhals and F. Kremer, *Journal*, 2003.
9. A. Brás, M. Dionísio, H. Huth, C. Schick and A. Schönals, *Physical Review E*, 2007, **75**, 061708.
10. Y. Shimizu, A. Kurobe, H. Monobe, N. Terasawa, K. Kiyohara and K. Uchida, *Chemical Communications*, 2003, 1676-1677.
11. L. Li, M. Salamończyk, S. Shadpour, C. Zhu, A. Jákli and T. Hegmann, *Nature communications*, 2018, **9**, 714.
12. L. Hanson, K. Clemons, D. Denning and D. Stevens, *Journal of medical and veterinary mycology*, 1995, **33**, 311-317.
13. H.-M. P. Chen, J. J. Ou and S. H. Chen, in *Nanoscience with Liquid Crystals*, ed. Q. Li Springer, 2014, ch. 6, pp. 179-208.
14. H. Iino, T. Usui and J.-i. Hanna, *Nature communications*, 2015, **6**, 6828.

15. W. Pisula, M. Zorn, J. Y. Chang, K. Müllen and R. Zentel, *Macromolecular rapid communications*, 2009, **30**, 1179-1202.
16. M. O'Neill and S. M. Kelly, *Advanced Materials*, 2011, **23**, 566-584.
17. O. Peeters, N. Blaton and C. De Ranter, *Acta Crystallographica Section C: Crystal Structure Communications*, 1996, **52**, 2225-2229.
18. W. McMillan, *Physical Review A*, 1972, **6**, 936.
19. C. Benmore, Q. Mou, K. Benmore, D. Robinson, J. Neuefeind, J. Ilavsky, S. Byrn and J. Yarger, *Thermochimica Acta*, 2016, **644**, 1-5.
20. N. Kapernaum and F. Giesselmann, *Physical Review E*, 2008, **78**, 062701.
21. S. Havriliak and S. Negami, *Polymer*, 1967, **8**, 161-210.
22. A. Hensel and C. Schick, *Journal of non-crystalline solids*, 1998, **235**, 510-516.
23. A. Dhotel, B. Rijal, L. Delbreilh, E. Dargent and A. Saiter, *Journal of Thermal Analysis and Calorimetry*, 2015, **121**, 453-461.
24. J. J. M. Ramos, R. Taveira-Marques and H. P. Diogo, *Journal of pharmaceutical sciences*, 2004, **93**, 1503-1507.
25. Z. Wojnarowska, K. Adrjanowicz, P. Włodarczyk, E. Kaminska, K. Kaminski, K. Grzybowska, R. Wrzalik, M. Paluch and K. Ngai, *The Journal of Physical Chemistry B*, 2009, **113**, 12536-12545.

Kinetic arrest of the end-over-end rotation controls the liquid-crystalline order in an organic glass prepared at different cooling rates, allowing systematic control of molecular packing for electronic applications.

